Available online at www.sciencedirect.com
SCIENCE DIRECT®
Nuclear Instruments and Methods in Physics Research A 498 (2003) 101–111
NUCLEAR INSTRUMENTS & METHODS IN PHYSICS RESEARCH Section A
www.elsevier.com/locate/nima

First results of the large COMPASS ^{6}LiD polarized target

J. Ball[a], G. Baum[b], P. Berglund[c], I. Daito[d], N. Doshita[e], F. Gautheron[b], St. Goertz[f], J. Harmsen[f], T. Hasegawa[g], J. Heckmann[f], N. Horikawa[d], T. Iwata[e,1], Yu. Kisselev[b], J. Koivuniemi[c], K. Kondo[e], J.M. Le Goff[a], A. Magnon[a], A. Meier[f], W. Meyer[f], E. Radtke[f], G. Reicherz[f], N. Takabayashi[e,*]

[a] *CEA Saclay, DAPNIA, 91191 Gif-sur-Yvette, France*
[b] *Physics Department, University of Bielefeld, 33501 Bielefeld, Germany*
[c] *Low Temperature Laboratory, P.O. Box 2200, Helsinki University of Technology, 02015, Finland, and Helsinki Institute of Physics, P.O. Box 64, University of Helsinki, Helsinki 00014, Finland*
[d] *CIRSE, Nagoya University, 464-8603 Nagoya, Japan*
[e] *Department of Physics, School of Science, Nagoya University, 464-8602 Nagoya, Japan*
[f] *Physics Department, University of Bochum, 44780 Bochum, Germany*
[g] *Faculty of Engineering, Miyazaki University, 889-2192 Miyazaki, Japan*

Received 10 December 2002; accepted 12 December 2002

Abstract

The COMPASS (NA58) experiment at CERN operates with a large solid polarized target (PT) to study the spin structure of the nucleon. The COMPASS PT system started its operation with the target material ^{6}LiD in 2001. Deuteron polarizations of $+54.2\%$ and -47.1% were achieved in a ^{3}He/^{4}He dilution refrigerator at a magnetic field of 2.5 T. The equal spin temperature (EST) concept was found to hold among the deuteron, the ^{6}Li and the ^{7}Li nuclei during the dynamic nuclear polarization (DNP) process. The agreement with the EST concept allows the permanent monitoring of only one nuclear species by the nuclear magnetic resonance (NMR) method.

PACS: 89.20.+a

Keywords: COMPASS; NA58; Polarized target; PT; DNP; Lithium deuteride

1. Introduction

The EMC result that the quarks carry unexpectedly a small fraction of the nucleon spin [1] has attracted the researchers and intensive experimental and theoretical work has been carried out to investigate the spin structure of the nucleon. The precise experiments in the 1990s, SMC at CERN, a series of experiments at SLAC, and HERMES at

*Corresponding author.
E-mail address: naoki.takabayashi@cern.ch (N. Takabayashi).
[1] Now at Department of Physics, Faculty of Science, Yamagata University, 990-8560 Yamagata, Japan.

0168-9002/03/$ - see front matter
doi:10.1016/S0168-9002(02)02116-2

DESY and the analysis with perturbative QCD evolutions show that the quarks carry 20–30% of the parent nucleon spin at $Q^2 = 10\ \mathrm{GeV}^2$ (There are many articles on this subject. For example [2]). Following these results, the gluon contribution $\Delta G/G$ to the nucleon spin is considered to be one of the candidates that might explain the spin puzzle and its direct measurement is awaited.

One of the main goals of the COMPASS experiment is to measure $\Delta G/G$ with the longitudinally polarized 100–190 GeV muon beam and the longitudinally polarized nucleons in a solid state target [3]. In parallel, the study of the strange quark spin via the Λ polarization measurement as well as further measurements of the longitudinal spin distribution functions can be performed. In addition, the COMPASS experiment allows the measurement of the transverse spin-dependent structure functions with a transversely polarized target.

In the COMPASS experiment, the measurement of $\Delta G/G$ is obtained by the photon–gluon fusion process and can be accessed by the experimental asymmetry

$$A^{\mathrm{exp}} = \frac{N_{c\bar{c}}^{\uparrow\downarrow} - N_{c\bar{c}}^{\uparrow\uparrow}}{N_{c\bar{c}}^{\uparrow\downarrow} + N_{c\bar{c}}^{\uparrow\uparrow}}, \tag{1}$$

where $N_{c\bar{c}}^{\uparrow\downarrow}$ ($N_{c\bar{c}}^{\uparrow\uparrow}$) is the counting rate of the open charm leptoproduction events for anti-parallel (parallel) spin orientation between the beam and the target.

Since the evaluation of $N_{c\bar{c}}^{\uparrow\downarrow}$ and $N_{c\bar{c}}^{\uparrow\uparrow}$ is based on the reconstruction from the decay particles of short living hadrons that contain a charm quark, e.g. $D^0 \to K^-\pi^+$, their multiple scattering should be minimized. Practically, the minimization of the materials around the target is essential for the experiment. The PT apparatus with the focus to this aspect is described in Section 2.

In first order, there is no difference in obtaining $\Delta G/G$ from a proton or a neutron. Therefore, the overall effective polarization in the target material is a key factor. In addition, the limited beam intensity and the small cross-section of open charm leptoproduction make it necessary to use a target of sufficient length in the beam direction. The advantage of ^{6}LiD over other PT materials is reviewed in Section 3. The material preparation and its mass production technique for the COMPASS experiment are reported in Section 4.

High deuteron polarization values of +54.2% and −47.1% with an average precision of absolute 1.0% were obtained. The polarization measurement inside the extended target cells and the polarization build-up with the frequency modulation technique are discussed in Section 5. The validity of the EST concept among the different spin species in the ^{6}LiD material is an important issue from the view of the hardware setup and the operation strategy on the target polarization monitoring which is crucial for the determination of $\Delta G/G$. In Section 6, the first results of the EST concept are reported.

2. Apparatus

The PT apparatus in the initial layout of the COMPASS experiment is based on the system build for the SMC (NA47) experiment [4,5]. The apparatus consists of a high cooling power dilution refrigerator, a superconducting magnet producing 2.5 T, two 70 GHz microwave systems for DNP and the NMR signal detection system for the polarization monitoring. In Fig. 1, the side view of the apparatus is shown.

However, there are some modifications concerning the materials inside the particle detection acceptance. Fig. 2 illustrates a detailed view on the target cells and the materials traversed by the produced particles. Due to the fixed helicity state of the muon beam, the double target cell configuration is employed, i.e. the target material in the two cells is polarized in the opposite direction to each other to cancel the false asymmetry due to time-dependent variations in the beam intensity. In the COMPASS experiment, the polarized muon beam is focused to a diameter of $\sigma_x \approx 8$ mm and $\sigma_y \approx 8$ mm. The target cell diameter is chosen to be 30 mm, while it was 50 mm in SMC, in order to reduce the multiple scattering of the produced particles in the target material itself. Each target cell has a cylinder shape with a length of 600 mm and they are separated by a 100 mm gap which is

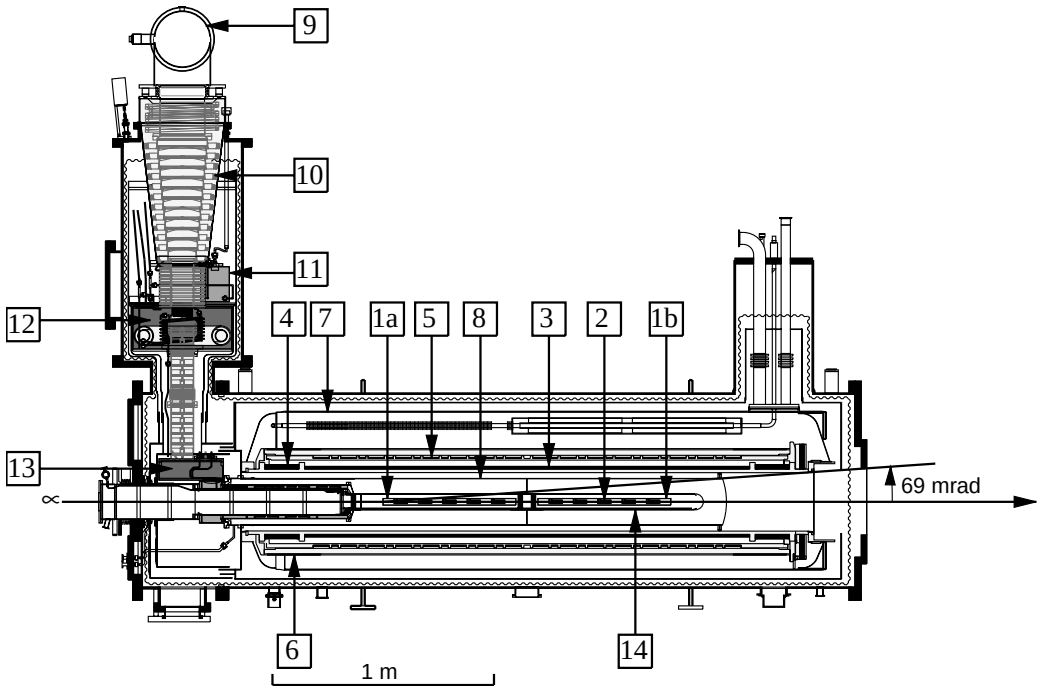

Fig. 1. Side view of the COMPASS PT apparatus. The muon beam traverses from left to right. The geometrical acceptance for the outgoing particles is 69 mrad in the opening angle from the upstream end of the target cell. (1a) upstream target cell, (1b) downstream target cell, (2) 10 NMR coils inside target material, (3) solenoid coil, (4) compensation coils, (5) 16 correction coils, (6) dipole coil, (7) liquid helium vessel for the magnet, (8) microwave cavity, (9) ^{3}He pumping port, (10) ^{3}He precooler, (11) separator, (12) evaporator, (13) still, and (14) mixing chamber.

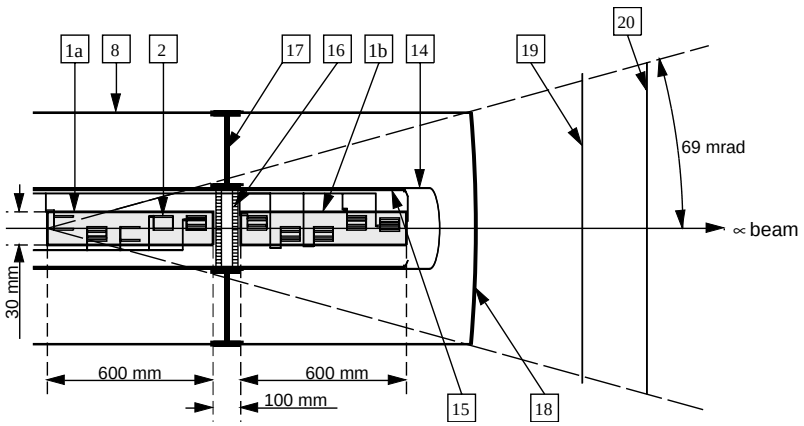

Fig. 2. Materials inside the particle detection acceptance including the essential modifications: the microwave stopper and the target cells. For better illustration, the vertical–horizontal scale is not proportional. (1a) upstream target cell, (1b) downstream target cell, (2) 10 NMR coils inside the target cells, (8) microwave cavity, main cylindrical structure, (14) mixing chamber (glass-fiber-epoxy, $t = 0.06$ mm), (15) target holder support, fitting inside the mixing chamber (kevlar-epoxy, $t = 0.83$ mm), (16) microwave absorbers (polyamid honeycomb with carbon coating) with the reflection mesh (Cu, $t = 0.05$ mm) on their surfaces, (17) microwave stopper (made of $t = 0.1$ mm Cu foil), (18) cavity end window (made of $t = 0.5$ mm Cu foil), (19) magnet radiation shield (Stainless steel, $t = 0.5$ mm), and (20) magnet vacuum window (Al, $t = 1$ mm). Here, t denotes the thickness of each material.

sufficient to identify by the vertex reconstructions in which cell the events of interest take place.

For simultaneous DNP with opposite signs in the two target cells, the microwave cavity has to be constructed appropriately. The microwave cavity which is fed by two 70 GHz microwave sources is separated into two halves with a microwave stopper made of 100 μm Cu foil. The skin depth at 70 GHz for high-conductivity copper assuming a residual resistance ratio of 100 between a room temperature and 1 K is less than 0.1 μm. Thus, the microwave leakage for a simple plane wave is expected to be less than 30 dB. The leakage through the central hole is prevented by the 100 mm long cylindrical part around the mixing chamber made of 100 μm Cu foil soldered to the separation window foil (see Fig. 2(17)). The gap between the mixing chamber and the cylindrical part is kept below one half of the wavelength to suppress the wave propagation. At room temperature an isolation of better than 20 dB between the two halves of the microwave cavity was measured with this configuration. The downstream end of the cavity has a window of 0.5 mm thick Cu (Fig. 2(18)). Compared to the SMC experiment, the thickness of material is considerably reduced. Table 1 summarizes the radiation length due to the materials in the detection acceptance.

Like in the SMC experiment, the spin reversal in the two target cells was performed in about 30 min by the so-called field rotation technique using combinatorial operation of the longitudinal solenoid field (2.5 T) and the transverse dipole field (0.5 T) [4–7]. The field rotation is done typically every 8–12 h in order to reduce the false asymmetry due to the time-dependent fluctuation in the spectrometer efficiency and due to the slightly different amount of material in the two cells. The measurements indicated negligibly small losses of the deuteron polarization in ^{6}LiD during the rotation procedures, which were performed in the frozen spin mode below 90 mK and at a minimum magnetic field of 0.5 T (see also Section 5).

For the polarization measurement, five NMR coils were embedded in each cell. The coils were made of 1.6 mm diameter non-magnetic CuNi tube with a wall thickness of 0.1 mm and with outer Teflon tube protection. They were wound in two-loop shape with a length of 70 mm and a distance of 10 mm between the halves. The coils were equally spaced and spirally mounted inside the target cells to probe equally different parts of the cell. A so-called Liverpool Q-meter [8] for phase sensitive detection of the NMR signals was connected to each NMR coil, forming a series LRC circuit tuned to 16.38 MHz, the deuteron Larmor frequency at 2.5 T. A detailed description of the NMR circuit is given in Ref. [5,8–11]. The deuteron NMR signals (see Section 5 and Fig. 4) were taken in 1–5 min intervals during the physics data taking.

Table 1
Thickness of the materials in the PT apparatus in radiation lengths X_0 for the outgoing particles with an opening angle of 69 mrad from the upstream end of the target cell. Such particles traverse a length of x(69 mrad) in each material described in Fig. 2. Generally, the total ratio x/X_0 varies depending on the vertex point and the outgoing angle

Material	Label in Fig. 2	X_0 (mm)	x(69 mrad) (mm)	x/X_0 (%)
^{3}He/^{4}He	—	6740	288	4.3
Mixing chamber	(14)	287	12	4.2
Target holder support	(15)	150	8.7	5.8
Microwave stopper	(17)	14.3	0.1	0.7
Cavity end window	(18)	14.3	0.5	3.5
Magnet radiation shield	(19)	17.6	0.5	2.8
Magnet vacuum window	(20)	88.9	1	1.1
Total				22.4

3. The choice of the polarized target material

Already in 1980 ^{6}LiD has been proposed as an attractive candidate for a polarized target material [12,13]. Its main advantages are (a) a large fraction of polarizable nucleons with respect to the total amount of nucleons per molecule and (b) a maximum polarization, which for both nuclei can be made as high as 50% at a magnetic field of 2.5 T. The result is an unrivaled high effective nucleon polarization P_{eff} of the molecule, the importance of which may be seen from the so-called target figure of merit:

$$F = \rho\kappa P_{\text{eff}}^2, \tag{2}$$

where the symbols ρ and κ denote the density and the packing factor of the material, respectively. The inverse of F is directly proportional to the measuring time, which is needed in order to achieve a certain statistical accuracy of the particle physics data.

During the last decade major improvements in the preparation method for this material have been achieved at Saclay, Bonn and Bochum, by which the maximum polarization at a given magnetic field could be considerably enhanced [14–19]. Furthermore, the material turned out to be very radiation hard being a suitable choice for experiments, where the energy deposit of the particle beam is large [16,17,20]. By these efforts, ^{6}LiD was not only used for nuclear physics experiments at PSI [21] and at Saclay [22] but also for the spin structure experiment at SLAC, in which an electron beam of high intensity was applied [20,23].

For the COMPASS experiment with its low particle flux (of the order of 10^7 muons/s in time average) the major advantage of ^{6}LiD over competing target materials is its large value of P_{eff}. This number is most easily determined for materials having only one polarizable nuclear species. Here P_{eff} is given by the product of the polarization P_{n} of the nucleons within the nucleus weighted by the fraction of polarizable nucleons in the molecule. This last number is usually called the dilution factor f. The nucleon polarization P_{n} itself is given by the product of the measured nuclear polarization P_{N} and the probability x for a parallel orientation of the nucleon spin with respect to that of the nucleus

$$P_{\mathrm{eff}} = P_{\mathrm{n}} f = x P_{\mathrm{N}} f. \tag{3}$$

For the deuteron, in which the proton and the neutron are in a S-state or in a D-state with probabilities of 95.1% and 4.9%, respectively, x is calculated to $0.926 \pm 0.016\%$ [24]. Consequently, for materials containing more than one kind of polarizable nuclei, the effective polarization is given by the sum of the individual contributions of the different species. For the ^{6}LiD molecule one obtains instead of Eq. (3):

$$P_{\mathrm{eff}} = x_{\mathrm{D}} P_{\mathrm{D}} f_{\mathrm{D}} + x_{^6\mathrm{Li}} P_{^6\mathrm{Li}} f_{^6\mathrm{Li}}. \tag{4}$$

Herein the small contribution of unsubstituted ^{7}Li, which amounts to about 5% for a highly enriched ^{6}Li metal, is ignored.

The ^{6}Li nucleus can be regarded as being composed of a spinless α particle plus a proton and a neutron carrying the total spin-1 of the nucleus. Unlike the deuteron the valence nucleons of ^{6}Li can be found also in a P-state to a certain extent. The value of $x_{^6\mathrm{Li}}$ has been calculated by Schellingerhout et al. [25] for nine different models of the three body (α, p, n) forces, eight of them giving rather similar results between 0.85 and 0.89 with an average of 0.866 ± 0.012. Since for ^{6}LiD the fractional dilution factors f_{D} and $f_{^6\mathrm{Li}}$ are both equal to 0.25 Eq. (4) simplifies to

$$P_{\mathrm{eff}} \simeq (x_{\mathrm{D}} + x_{^6\mathrm{Li}}) f \; P_{\mathrm{N}} = 0.22, \tag{5}$$

wherein to a good approximation also both polarizations are assumed to be equal with a value of 50% (for a justification see Section 6). Table 2 shows a comparison of the important quantities for all materials in question. The respective polarizations are taken from the SMC experiment, which featured a polarized target setup similar to the COMPASS experiment. As a result the figure of merit of ^{6}LiD is the largest of all possible materials and even a factor 1.8 higher than that of ammonia (NH_3) as the second best choice.[2]

4. Preparation of ^{6}LiD

In order to use ^{6}LiD for the COMPASS experiment, the particular challenge was the development of a mass production technique, which ensured the preparation of about 0.5 kg of highly polarizable granules of this material [18,19]. A first step was the synthesis of the material from highly enriched ^{6}Li ($\approx 95.5\%$) and pure deuterium gas ($\approx 99.8\%$) by the reaction

$$2\mathrm{Li} + \mathrm{D}_2 \rightarrow 2\mathrm{LiD},$$

which was performed in a specially designed furnace at temperatures between 700 and 1100 K.

[2] Actually, it is foreseen to use NH_3 in a later phase of the COMPASS experiment. Together with the data from ^{6}LiD this will open up the possibility to determine the gluon contribution to the proton and the neutron spin separately.

After slowly cooling down and removing the material from the reaction chamber it was cut into small crystals with typical dimensions of a few millimeters. In order to allow the DNP mechanism to operate, a suitable amount (10^{-4}–10^{-3} per nucleus) of paramagnetic centers, i.e. of unpaired electrons, has to be implanted into the material. For this purpose the granules were exposed to the 20 MeV electron beam of the Bonn injection linac in batches of about 70 cm^3, each for several hours. During the irradiation, in which each sample received a total dose of 2×10^{17} e^-/cm^2, the material was kept at a temperature of 190 ± 1 K by means of a special irradiation cryostat [18]. The paramagnetic resonance of samples from each of the 13 batches were studied in a conventional X-band EPR spectrometer operating at 9.35 GHz. In order to prevent the paramagnetic centers from decaying, these studies as well as the storage of the material required the use of low (liquid nitrogen)

Table 2
Comparison of the figure of merit among ^{6}LiD and selected common polarized target materials. The nuclear polarization and the packing factor represent the typical values. The density of NH_3, butanol and deuterated butanol (d-butanol) is taken from Ref. [5]. For the clear demonstration of the advantage of ^{6}Li, the small contribution of ^{7}Li is ignored and the nuclear polarizations of both the deuteron and the ^{6}Li nuclei are assumed to be 50%. The very small contribution of the nitrogen polarization in ammonia is ignored as well

		NH_3	Butanol	d-Butanol	^{6}LiD
Polarization of the nuclei	P_N	H: 0.90	H: 0.90	D: 0.50	D, ^{6}Li: 0.50
Polarization of the nucleons	P_n	0.90	0.90	0.463	0.463 in D 0.433 in ^{6}Li
(fractional) Dilution factor	f	0.176	0.135	0.238	D, ^{6}Li: 0.25
Effective polarization	P_{eff}	0.158	0.122	0.110	0.224
Density (g/cm^3)	ρ	0.85	0.99	1.10	0.84
Packing factor	κ	0.60	0.60	0.60	0.55
Figure of merit (10^{-3} g/cm^3)	F	12.7	8.8	8.0	23.2

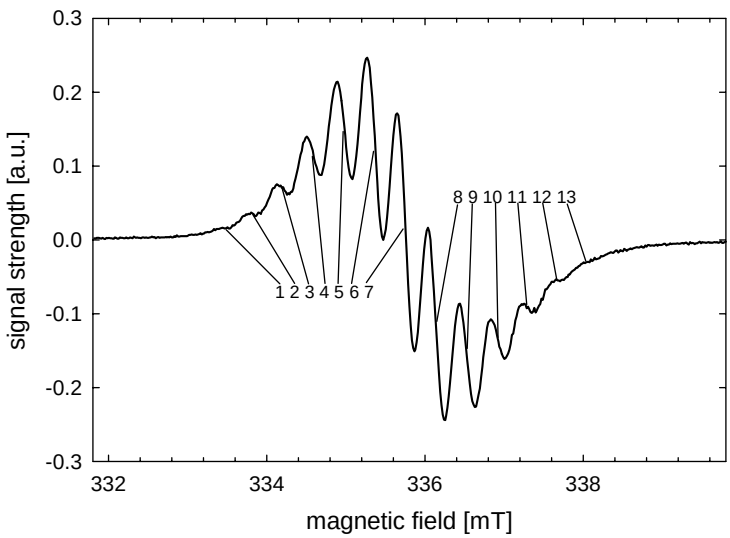

Fig. 3. EPR signal of electron irradiated ^{6}LiD. The 13 individual lines belong to the respective total magnetic quantum number of the six adjacent ^{6}Li nuclei.

temperatures. It was found that the radiation dose mentioned above give rise to a concentration of paramagnetic centers of $2 \times 10^{19}/\mathrm{g}$ and that the resonance structure of these defects is in agreement with the model of so called F-center. It consists of a vacancy in the anion sub-lattice, in which a free electron is captured. The wave function of the electron extents over the lattice sites of the six adjacent ^{6}Li nuclei, which leads to a characteristic 13 line pattern of the EPR signal as shown in Fig. 3.

5. Deuteron polarization

The calibration of the deuteron, the ^{6}Li, and the ^{7}Li polarizations were done by the thermal equilibrium (TE) method, in which the respective NMR signals at the nominal field of 2.5 T are taken in the evaporative ^{4}He-mode of the refrigerator at temperatures of 0.97 and 1.44 K. Fig. 4(a) shows a characteristic deuteron spectrum obtained under these conditions, which corresponds to a polarization of about 0.05%. On the other hand the thermal equilibrium polarization P_{TE} can be calculated by means of the Brillouin function B_I

$$P_I = B_I\left(\frac{\mu B}{k_{\mathrm{B}}T}\right), \tag{6}$$

which—at given temperature T and magnetic field B—only depends on the spin quantum number I and the magnetic moment μ of the respective nucleus. Since the nuclear polarization is proportional to the integral intensity of the NMR spectra, the enhanced nuclear polarization P_{dyn} is then determined by comparing the intensity A_{dyn} of the dynamic signals to the intensity A_{TE} of the TE signals according to the formula:

$$P_{\mathrm{dyn}} = \frac{A_{\mathrm{dyn}}}{A_{\mathrm{TE}}} P_{\mathrm{TE}}. \tag{7}$$

For the process of dynamical polarization the refrigerator is operated in the ^{3}He/^{4}He dilution mode at temperatures between 80 and 300 mK depending on the actual microwave power. A typical build-up curve of the deuteron polarization is shown in Fig. 5. Polarizations of +40% and −35% are usually reached within 1 day at

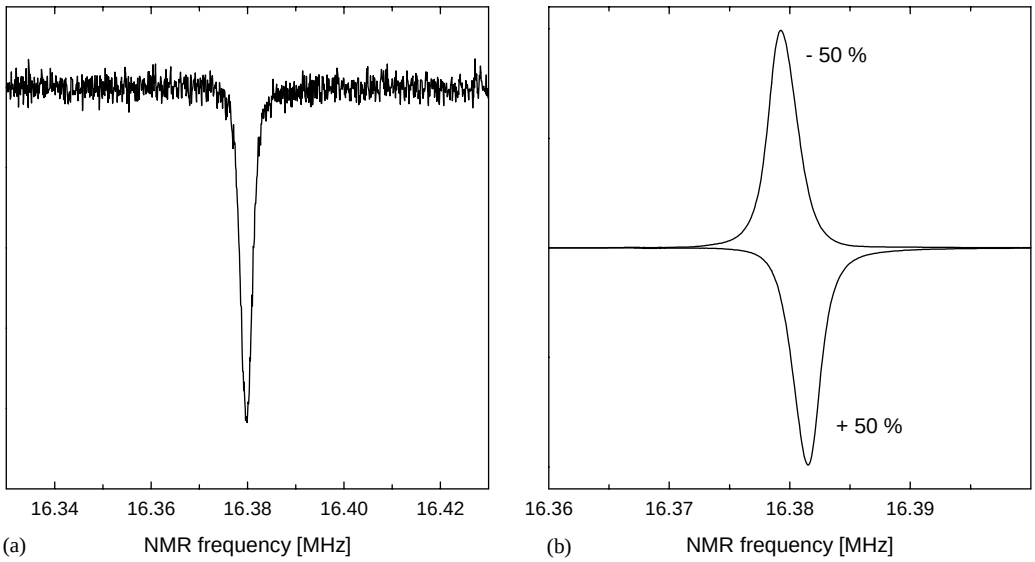

Fig. 4. (a) Thermal equilibrium signal at 0.97 K and (b) dynamical signals with $|P| \simeq 50\%$ of the deuteron in ^{6}LiD taken with coil No. 8 (downstream cell). All NMR signals were recorded within a frequency range of 100 kHz. In (b) only the inner 40 kHz part of the NMR window is shown, in order to exhibit more clearly the polarization-dependent shift of the signal.

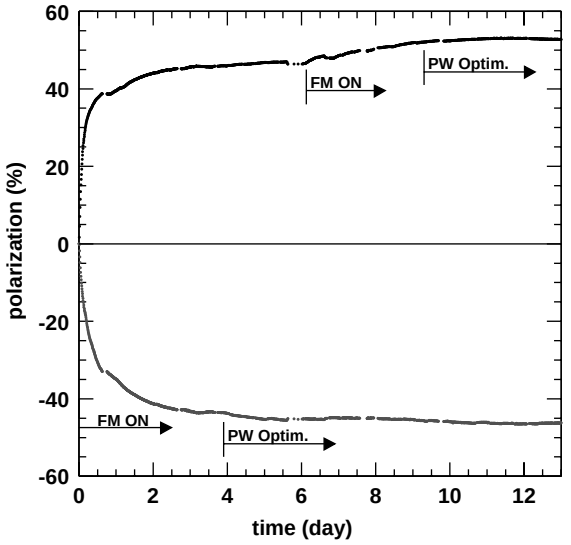

Fig. 5. Example of the deuteron polarization build-up. The upstream (downstream) cell is polarized positively (negatively). The interruptions of the data points correspond to a magnetic field rotation or to a technical interruption of the NMR data taking. The start time of the microwave frequency modulation is indicated by 'FM-ON' and that of the microwave power optimization by 'PW Optim'.

comparatively high values of the microwave power, whereas a period of about 1 week is needed for obtaining the full polarization. During this second stage it is preferable to reduce the microwave power in order optimize the working temperature of the refrigerator. The final deuteron polarizations (averaged over all NMR coils) were measured to be +54.2% and −47.1%. They were obtained under a modulation of the microwave frequency with a frequency of 500 Hz and a peak to peak amplitude of about 20 MHz. This technique is already known from the SMC experiment as being helpful in order to maximize the achievable polarization [5,26,27].

Fig. 4(b) shows two dynamic NMR signals of coil No. 8 with polarizations of about +50% and −50%. In contrast to the TE signals, the dynamic signals exhibit a slight but easily detectable asymmetry around their respective centers, which themselves are shifted towards lower ($P<0$) or towards higher ($P>0$) frequencies. The magnitude of both, the asymmetry and the frequency shift depend on the sign as well as on the degree of the polarization. Qualitatively this effect can be explained by different local fields at the sites of the deuterons, which are produced by the polarization of the neighboring ^{6}Li nuclei [28,29].

During the polarization build-up a shift of the optimum microwave frequencies towards the center of the electron Larmor resonance was observed. In the case of unmodulated microwaves the optimum values started from about 70.210 and 70.270 GHz for positive and negative polarizations, respectively. The final frequencies were set around 70.238 and 70.245 GHz for $|P|>40\%$. This behavior is qualitatively in agreement with the predictions following from the low-temperature treatment of the spin temperature theory for hyperfine broadened electron spin systems [30]. In the case of enabled frequency modulation the polarization-dependent shift was observed to be slightly less pronounced than without modulation. Compared to the target materials used in the SMC experiment [5], the polarization build-up of lithium deuteride is considerably slower. This observation is attributed to the relatively long relaxation time T_1 of the paramagnetic F-center. Due to the technique of spin reversal by field rotation the long build-up time of ^{6}LiD is not a serious drawback regarding the accuracy of the COMPASS experiment, which relies on frequent changes of the relative orientation of the polarizations in the two target cells with respect to the muon beam. Most of the interruptions of the data points in Fig. 5 correspond to these field rotation cycles, which are performed in the frozen spin mode. Compared to butanol and ammonia the much larger nuclear relaxation time of lithium deuteride at low magnetic fields—being about 2000 h at 0.5 T and at 90 mK—prevents the material from any polarization loss during the procedure of polarization reversal.

The individual polarizations as measured with each of the 10 NMR coils are shown in Table 3. They are differing by amounts larger than the measurement errors. Thus, we consider that they reflect the physical polarizations as present at the different positions within the target cells. One explanation for these differences considered so far could be ruled out by a comparison with the

Table 3
Maximum deuteron polarization. The NMR coils are numbered from upstream to downstream in an ascending order. The major part of the error is from the TE calibration. The variation of the measured polarization among the coils is discussed in the text. The average polarization is +54.2% in the upstream cell and −47.1% in the downstream cell

Upstream cell		Downstream cell	
NMR coil	$P_D \pm \Delta P_D$	NMR coil	$P_D \pm \Delta P_D$
1	$+57.8 \pm 2.2$	6	-46.2 ± 0.9
2	$+52.1 \pm 0.5$	7	-48.3 ± 0.8
3	$+53.0 \pm 0.9$	8	-49.6 ± 0.7
4	$+51.3 \pm 1.3$	9	-45.5 ± 0.8
5	$+56.7 \pm 1.0$	10	-45.9 ± 1.0

preliminary polarization results from the present run of 2002, which show similar differences between the NMR coils. After emptying and refilling the target cells a possible correlation between a certain NMR coil and a certain production lot, which may have been prepared under slightly different conditions, is now to be excluded. The only explanations left are based on variations of either the temperature or of the microwave frequency and power distribution along the two target cells. For instance, a $\pm 3 \times 10^{-5}$ inhomogeneity of the solenoid magnetic field leads to variation of the optimum frequency by 4 MHz. A detuning of that size may be already critical in achieving the highest possible polarization in this material. But also the power distribution within the microwave cavity may vary along the cavity axis due to the presence of differently absorbing or reflecting materials within the mixing chamber (e.g. the microwave stopper separating the two target cells).

It should be mentioned that a difference up to 7% between the average positive and negative polarizations has been observed, the sign of which is consistent with other results on ^{6}LiD samples of equal performance [15]. From the fact that a similar result has also been observed using the Bochum test cryostat—a dilution refrigerator with a completely different geometry of the mixing chamber—it is believed that this effect is due to an inherent property of the material as prepared in the way described above.

6. Validity of the equal spin temperature (EST) concept

Not only the polarization of the deuteron, but also that of ^{6}Li and that of the residual ^{7}Li nuclei ($\approx$4.5%) are of importance for the evaluation of the particle physics data as well as for the understanding of the DNP process. These polarizations are plotted versus the deuteron polarization in Fig. 6 together with the prediction by the EST concept [30]. The basic statement of this concept is that the Zeeman system of every nuclear species with spin I present in the material share the same spin temperature T_S. In other words the difference of the Zeeman occupation numbers and thus the polarization of the particular spin system can be calculated from the respective Brillouin function (6) with T replaced by T_S.

The NMR measurements of ^{6}Li and ^{7}Li were done by stopping the microwave pumping occasionally during the DNP process and by setting the solenoid field so that the Larmor frequency of ^{6}Li or ^{7}Li became equal to the NMR circuit resonance frequency, i.e. to 16.38 MHz. The correction coils, which are used to achieve the highest possible

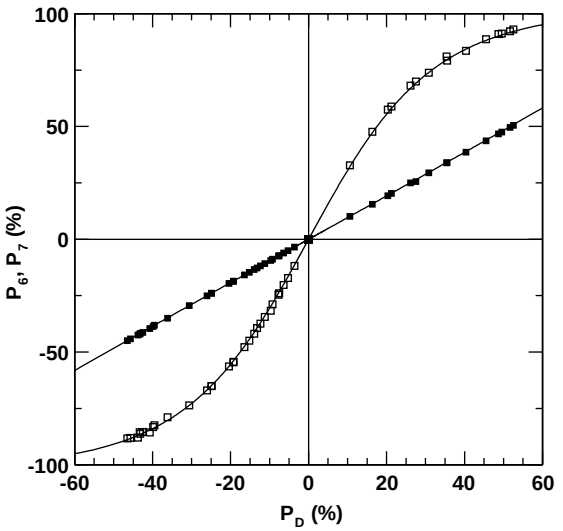

Fig. 6. The polarizations of the ^{6}Li and the ^{7}Li nuclei versus that of the deuteron. The closed (open) squares are the measured polarization of ^{6}Li (^{7}Li). The lines are the prediction by EST concept. The measurements are consistent with the EST concept.

homogeneity of the magnetic field, were adjusted according to the respective solenoid field. Before and after each measurement of the polarization of the two lithium isotopes the deuteron NMR signals were taken at the nominal field to verify that no polarization was lost. Just like in the case of the deuteron the polarizations of ^{6}Li and ^{7}Li were determined by the area method with the TE signals taken at 0.97 and at 1.44 K. It should be noted that the hardware tuning of the NMR system was kept unchanged throughout the experiment. Our data are in good agreement with the EST concept indicating a common spin temperature below 1 mK at the highest polarizations. Besides important information about the DNP process the observed agreement offers significant practical benefits. Most importantly, it is not necessary to measure the polarizations of all the different spin species separately, which would either require more NMR coils in the material or a frequent change of the magnetic field in order to use the existing coils for the polarization measurement of the other nuclei. Both solutions would imply negative consequences for the efficiency of the particle physics experiment. With the validity of the EST concept it is sufficient to monitor one of the nuclear polarizations, whereby all of the NMR coils can be used to check the uniformity of the polarization section by section. The corresponding polarization values of the other nuclei may then be calculated most simply using Eq. (6).

7. Conclusion

The COMPASS PT system successfully started its operation with the target material ^{6}LiD. In order to provide the needed large amount of this material, reliable techniques for its production and irradiation have been developed. By means of systematic EPR studies it could be shown that the resonance line of the DNP active paramagnetic center is consistent with the atomic structure of the F-center. The optimum concentration of these centers was determined to $2 \times 10^{19}/\mathrm{cm}^3$. Deuteron polarizations of $+54.2\%$ and -47.1% were achieved at a magnetic field of 2.5 T using the technique of frequency modulation. The optimum microwave frequencies were observed to vary with increasing polarization in agreement with the theory of DNP for hyperfine broadened EPR lines. It was found that the EST concept holds among the deuteron, the ^{6}Li, and the ^{7}Li nuclei during the DNP process.

Acknowledgements

We are indebted to the Chemistry Department of the University of Bochum for their expertise in the material development. We received various essential supports from CERN LHC/ECR Division for the cryogenic installations. We sincerely thank Saclay DAPNIA STCM and SIG Division and CERN EP/TA3 Division for their helps in the magnet installation. The professional works by the COMPASS technicians, J.M. Demolis and V. Pesaro, are gratefully acknowledged. The corresponding author would like to thank the Japanese colleagues in the COMPASS collaboration for their stimulations.

References

[1] J. Ashman, et al., Nucl. Phys. B 328 (1989) 1.
[2] M. Anselmino, A. Efremov, E. Leader, Phys. Rep. 261 (1995) 1;
J. Ellis, M. Karliner, Phys. Lett. B 341 (1995) 397.
[3] COMPASS Proposal, CERN/SPSLC 96-14, SPSLC/P297, 1 March 1996.
[4] J. Kyynäräinen, Nucl. Instr. and Meth. A 356 (1995) 47.
[5] D. Adams, et al., Nucl. Instr. and Meth. A 437 (1999) 23.
[6] A. Daël, D. Cacaut, H. Desportes, R. Duthil, B. Gallet, F. Kircher, C. Lesmond, Y. Pabot, J. Thinel, IEEE Trans. Magn. 28 (1992) 560.
[7] J.M. Le Goff, et al., Nucl. Instr. and Meth. A 356 (1995) 96.
[8] G.R. Court, D.W. Gifford, P. Harrison, W.G. Heyes, M.A. Houlden, Nucl. Instr. and Meth. A 324 (1993) 433.
[9] T.O. Niinikoskii, Nucl. Instr. and Meth. A 356 (1995) 62.
[10] Y.K. Semertzidis, Nucl. Instr. and Meth. A 356 (1995) 83.
[11] Yu.F. Kisselev, Phys. Part. Nucl. 31 (2000) 354.
[12] A. Abragam, V. Bouffard, Y. Roinel, P. Roubeau, J. Phys. (Paris) L 41 (1980) 309.
[13] V. Bouffard, Y. Roinel, P. Roubeau, A. Abragam, J. Phys. (Paris) 41 (1980) 1447.
[14] P. Chaumette, J. Derégel, G. Durand, J. Fabre, I. van Rossum, High energy spin physics, in: K.J. Heller (Ed.), Proceedings of the Eighth International Symposium,

Minneapolis, 1988, AIP Conference Proceeding, Vol. 2, AIP, New York, 1989, p. 1275.
[15] B. van den Brandt, J.A. Konter, S. Mango, M. Weßler, High energy spin physics, in: W. Meyer, E. Steffens, W. Thiel (Eds.), Proceedings of the Ninth International Symposium, Bonn, 1990, Springer, Berlin, 1991, p. 320.
[16] St. Goertz, Ph.D. Thesis, Universität Bonn, BONN-IR-95-08.
[17] St. Goertz, et al., Nucl. Instr. and Meth. A 356 (1995) 20.
[18] A. Meier, Ph.D. Thesis, Universität Bochum, 2001.
[19] St. Goertz, Habilitation, Universität Bochum, 2002.
[20] S. Bültmann, et al., Nucl. Instr. and Meth. A 425 (1999) 23.
[21] S. Ritt, et al., Phys. Rev. C 43 (1991) 745.
[22] J. Ball, et al., Nucl. Instr. and Meth. A 381 (1996) 4.
[23] E155 Collaboration, P.L. Anthony, et al., Phys. Lett. B 458 (1999) 529;
E155 Collaboration, P.L. Anthony, et al., Phys. Lett. B 458 (1999) 536;
E155 Collaboration, P.L. Anthony, et al., Phys. Lett. B 463 (1999) 339.
[24] O.A. Rondon, Phys. Rev. C 60 (1999) 035201.
[25] N.W. Schellingerhout, et al., Phys. Rev. C 48 (1993) 2714.
[26] Yu.F. Kisselev, Nucl. Instr. and Meth. A 356 (1995) 99.
[27] B. Adeva, et al., Nucl. Instr. and Meth. A 372 (1996) 339 Erratum B. Adeva, et al., Nucl. Instr. and Meth. A 376 (1996) 490.
[28] A. Abragam, M. Chapellier, J.F. Jacquinot, M. Goldman, J. Magn. Resonance 10 (1973) 322.
[29] Y. Roinel, V. Bouffard, J. Magn. Resonance 18 (1975) 304.
[30] A. Abragam, M. Goldman, Rep. Prog. Phys. 41 (1978) 395.